

## **<sup>68</sup>Ga-Pentixafor PET/CT for imaging of chemokine receptor-4 expression in Waldenström macroglobulinemia/lymphoplasmacytic lymphoma: comparison to <sup>18</sup>F-FDG PET/CT**

<sup>1,2</sup>Yaping Luo\*, <sup>3</sup>Xinxin Cao\*, <sup>1,2</sup>Qingqing Pan, <sup>3</sup>Jian Li, <sup>3</sup>Jun Feng, <sup>1,2</sup>Fang Li†

<sup>1</sup>Department of Nuclear Medicine, <sup>3</sup>Department of Hematology  
Chinese Academy of Medical Sciences and Peking Union Medical College Hospital;  
<sup>2</sup>Beijing Key Laboratory of Molecular Targeted Diagnosis and Therapy in Nuclear  
Medicine

### **†Corresponding Author:**

Fang Li  
Department of Nuclear Medicine  
Chinese Academy of Medical Sciences and Peking Union Medical College Hospital;  
Beijing Key Laboratory of Molecular Targeted Diagnosis and Therapy in Nuclear  
Medicine  
Wangfujing, Dongcheng District, Beijing 100730, P.R. China  
Email: lifang@pumch.cn  
Telephone: 86-10-69155502

### **First Author:**

1. Yaping Luo (fellow)  
Department of Nuclear Medicine  
Chinese Academy of Medical Sciences and Peking Union Medical College Hospital  
Wangfujing, Dongcheng District, Beijing 100730, P.R. China  
Email: luoyaping@livecom  
Telephone: 86-10-69157034

2. Xinxin Cao (associate professor)

Department of Hematology

Chinese Academy of Medical Sciences and Peking Union Medical College Hospital;

Wangfujing, Dongcheng District, Beijing 100730, P.R. China

Email: caoxinxin@126.com

Telephone: 86-10-69155027

\*Contributed equally to this work.

Word Count: 4998

This work was supported by the National Natural Science Foundation of China

(81701741), CAMS Initiative for Innovative Medicine (CAMS-I2M, 2017-I2M-3-001),

and the Fundamental Research Funds for the Central Universities, the Young Scientific

Research Fund of PUMC (2017320004).

**Running title:**  $^{68}\text{Ga}$ -Pentixafor PET/CT in WM/LPL

## ABSTRACT

$^{18}\text{F}$ -FDG PET/CT has some limitations in the evaluation of Waldenström macroglobulinemia/lymphoplasmacytic lymphoma (WM/LPL), an indolent B-cell lymphoma that primarily involves the bone marrow. Since there is a high level of chemokine receptor-4 expression in the B cells of WM/LPL patients, we performed a prospective cohort study to evaluate the performance of  $^{68}\text{Ga}$ -Pentixafor, which targets chemokine receptor-4 in WM/LPL, and compared it to the performance of  $^{18}\text{F}$ -FDG.

**Methods:** Seventeen patients with WM/LPL were recruited. All patients underwent both  $^{68}\text{Ga}$ -Pentixafor and  $^{18}\text{F}$ -FDG PET/CT. A positive PET/CT was defined as the presence of focal PET-positive lesions or diffuse bone marrow patterns (uptake >liver). The positive rates of the PET/CT scans of bone marrow, lymph nodes and other extramedullary involvement were statistically compared. **Results:**  $^{68}\text{Ga}$ -Pentixafor PET/CT had a higher positive rate than  $^{18}\text{F}$ -FDG PET/CT (100% vs. 58.8%,  $p = 0.023$ ) in the recruited WM/LPL patients. The sensitivities in detecting bone marrow involvement with  $^{68}\text{Ga}$ -Pentixafor and  $^{18}\text{F}$ -FDG PET/CT were 94.1% and 58.8%, respectively ( $p =$

0.077). In terms of detecting lymph node involvement,  $^{68}\text{Ga}$ -Pentixafor PET/CT showed a significantly higher positive rate than  $^{18}\text{F}$ -FDG PET/CT (76.5% vs. 11.8%,  $p = 0.003$ ).

In addition,  $^{68}\text{Ga}$ -Pentixafor also detected more paramedullary and central nervous system involvement than  $^{18}\text{F}$ -FDG. **Conclusions:**  $^{68}\text{Ga}$ -Pentixafor might be a promising imaging agent in the assessment of WM/LPL.

**KEY WORDS:**

Waldenström macroglobulinemia, lymphoplasmacytic lymphoma, CXCR4,

$^{68}\text{Ga}$ -Pentixafor, PET/CT

Waldenström macroglobulinemia/lymphoplasmacytic lymphoma (WM/LPL) is an uncommon indolent non-Hodgkin lymphoma characterized by the accumulation of lymphoplasmacytic cells in the bone marrow with excess production of monoclonal immunoglobulin.  $^{18}\text{F}$ -FDG PET/CT, a standard technique in the diagnosis and management of several types of tumors, has a limited role in diagnosing WM/LPL.

According to the consensus recommendations of the International Conference on Malignant Lymphoma,  $^{18}\text{F}$ -FDG PET/CT is recommended for the routine staging of FDG-avid, nodal lymphomas and is as the gold standard in essentially all histologies but not indicated in WM/LPL, unless there is a suspicion of aggressive transformation (*1*).

Data on  $^{18}\text{F}$ -FDG PET/CT for WM/LPL are very limited. A study on the role of  $^{18}\text{F}$ -FDG PET/CT imaging for WM showed that only 43% of patients had abnormal bone marrow uptake (*2*) despite bone marrow being the primary site of involvement.

Chemokine receptor-4 (CXCR4) is a key factor for tumor growth and metastasis and is expressed at a high density in at least 20 different types of solid cancers and hematopoietic malignancies (*3*).  $^{68}\text{Ga}$ -Pentixafor, a novel PET tracer with high affinity for

CXCR4, has recently been introduced in the assessment of several lymphoproliferative diseases, e.g., multiple myeloma, diffuse large B-cell lymphoma, and acute myeloid leukemia (4-7). Studies have shown a high level of CXCR4 expression in the B cells of patients with WM/LPL compared to B cells from healthy donors (8,9), which makes it possible for WM/LPL to be imaged with  $^{68}\text{Ga}$ -Pentixafor. We previously reported data from a patient with WM in whom  $^{68}\text{Ga}$ -Pentixafor PET/CT showed intense radioactivity in the bone marrow and lymph nodes that was superior to  $^{18}\text{F}$ -FDG PET/CT (10). In this study, we further aimed to evaluate the performance of  $^{68}\text{Ga}$ -Pentixafor PET/CT in WM/LPL in comparison with  $^{18}\text{F}$ -FDG PET/CT, which served as a reference.

## **MATERIAL AND METHODS**

### **Study Design and Patients**

This is a preliminary report of an ongoing prospective study evaluating the role of  $^{68}\text{Ga}$ -Pentixafor PET/CT in WM/LPL that was approved by the institutional review board of Peking Union Medical College Hospital (protocol #ZS-1113) and registered at Clinicaltrial.gov (NCT 03436342). To compare differences between imaging techniques, the endpoint was the positive rate of  $^{68}\text{Ga}$ -Pentixafor and  $^{18}\text{F}$ -FDG PET/CT for WM/LPL

in this preliminary study. A total of 17 patients diagnosed with WM/LPL in the Department of Hematology of the Peking Union Medical College Hospital were consecutively recruited from April 2017 to November 2018. Written informed consent was obtained from each patient. The clinical history and laboratory test results related to WM/LPL were recorded at enrollment in the study. Patients were then referred for  $^{18}\text{F}$ -FDG and  $^{68}\text{Ga}$ -Pentixafor PET/CT for evaluation of the disease, which were carried out within 1 week after enrollment. The imaging characteristics were analyzed afterwards.

### **PET/CT Imaging**

The radiolabeling of  $^{68}\text{Ga}$ -Pentixafor was performed manually immediately before injection. Briefly, 45  $\mu\text{L}$  sodium acetate (1.25 M) was added to 1 mL  $^{68}\text{GaCl}_3$  eluent ( $^{68}\text{Ga}^{3+}$  in 0.5 M HCl) obtained from a  $^{68}\text{Ge}/^{68}\text{Ga}$  generator (ITG, Germany) to adjust the pH to 3.5-4.0. After the addition of an aliquot of 20  $\mu\text{l}$  (1  $\mu\text{g}/\mu\text{l}$ ) DOTA-CPCR4-2 (CSBio Co, CA94025, USA), the mixture was heated to 105  $^{\circ}\text{C}$  for 15 min. The reaction solution was diluted to 5 ml and passed through a preconditioned Sep-Pak C18 Plus Light

cartridge (Waters, USA), and the cartridge was eluted with 0.5 ml 75% ethanol to obtain the final product. The radiochemical purity of the product was analyzed by thin-layer chromatography. The  $^{68}\text{Ga}$ -Pentixafor injections were filtered through a 0.22  $\mu\text{m}$  Millex-LG filter (EMD Millipore) before clinical use.

$^{18}\text{F}$ -FDG was synthesized in-house with an 11 MeV cyclotron (CTI RDS 111, Siemens, Germany).

The PET scans were performed on dedicated PET/CT scanners (Biograph 64 Truepoint TrueV, Siemens, Germany; Polestar m660, SinoUnion, China). In 12 patients, the PET/CT scans of the same patient were performed on the same scanner, while 3 patients underwent PET/CT scans with different scanners. Two patients underwent  $^{18}\text{F}$ -FDG PET/CT at outside hospitals. For  $^{18}\text{F}$ -FDG PET/CT, the patients fasted for over 6 h, and the blood glucose levels were monitored (4.7-6.9 mmol/L) prior to an injection of  $^{18}\text{F}$ -FDG (5.55 MBq/kg). The PET/CT images (2 min/bed) were acquired with an uptake time of  $68.5 \pm 12.1$  min (range 47-89 min). For  $^{68}\text{Ga}$ -Pentixafor PET/CT, imaging was performed (2-4 min/bed) with an uptake time of  $47.8 \pm 18.6$  min (range 30-90 min)



after an injection of  $84.6 \pm 26.2$  MBq (range 37.0-136.9 MBq)  $^{68}\text{Ga}$ -Pentixafor. The emission scan was obtained from the tip of the skull to the mid-thigh. All patients underwent unenhanced low-dose CT (120 kV, 30-50 mAs) for attenuation correction and anatomical reference. The acquired data were reconstructed using the ordered-subset expectation maximization method (Siemens Biograph 64: 2 iterations, 8 subsets, Gaussian filter, image size 168\*168; SinoUnion Polestar: 2 iterations, 10 subsets, Gaussian filter, image size 192\*192).

### **Image Interpretation and Statistical Analysis**

Two experienced nuclear medicine physicians (YL and QP) visually assessed the PET/CT images and were in consensus for the image interpretation. As WM/LPL primarily involves the bone marrow, the distribution and intensity of bone marrow uptake was regarded as the main imaging characteristic. The presence and sites of the lymph nodes and other extramedullary involvement were also recorded. For  $^{18}\text{F}$ -FDG, the intensity of the bone marrow uptake and uptake in extramedullary lesions was based on the 5-point Deauville score scale, which is widely used in lymphoma. For

$^{68}\text{Ga}$ -Pentixafor, the intensity of involvement was classified as mild, moderate and intense with the liver and spleen taken as the reference (mild: uptake  $\leq$  liver; moderate: liver < uptake  $\leq$  spleen; intense: uptake > spleen). Positive bone marrow involvement was defined as the presence of focal PET positive lesions (circumscribed focus  $\geq$  5 mm with increased radioactivity compared with the background uptake in bone marrow) or diffuse bone marrow patterns (homogeneous bone marrow uptake) with the following interpretation criteria: for  $^{18}\text{F}$ -FDG, a score of 4 for the bone marrow uptake was set as a positive cutoff based on the high interobserver concordance in a study on the visual descriptive criterion of multiple myeloma (11); and for  $^{68}\text{Ga}$ -Pentixafor, moderate or intense uptake was defined as being positive. The presence of positive lymph nodes and other extramedullary involvement was defined as uptake  $\geq$  score of 4 in  $^{18}\text{F}$ -FDG PET and moderate or intense uptake in  $^{68}\text{Ga}$ -PentixaforPET. The McNemar test was used to statistically compare the positive rates of  $^{68}\text{Ga}$ -Pentixafor and  $^{18}\text{F}$ -FDG PET/CT. A  $p$ -value <0.05 was considered statistically significant.

## RESULTS

### Clinical Characteristics

Seventeen patients with WM/LPL (11 male, 6 female; age,  $62.6 \pm 10.5$  yr, range 48-87 yr) were enrolled in this study. Fifteen patients had newly diagnosed WM/LPL (1 patient with smoldering WM), and 2 patients had relapsed disease (patient #3, 5). Anemia was found in 14/17 (82.4%) patients, and 2/17 (11.8%) patients had thrombocytopenia. The median proportion of infiltrated lymphoplasmacytic cells found from bone marrow aspiration was 8.75% (range, 2.5%-31.0%). Peripheral neuropathy, which is one of the common disorders induced by paraprotein in WM/LPL, was found in 3/17 (17.6%) patients (patient #3, 4, 9). One patient (patient #4) had Bing-Neel syndrome (WM involving the central nervous system). Two patients (patient #6, 11) had secondary amyloidosis due to WM/LPL. According to the International Scoring System for WM proposed in 2009 (12), 7 patients were classified as high risk and 7 patients were intermediate risk. Two patients were at low risk. One patient with IgD  $\kappa$  LPL (patient #13) had an unknown risk stratification as the serum M-protein and  $\beta 2$ -microglobulin levels were not measured; in addition, the International Scoring System for WM may not be expanded enough to include to the risk stratification of IgD LPL. Mutation of myeloid

differentiation primary response 88, which has been identified in >90% of WM/LPL patients by whole-genome sequencing (13), was documented in all patients in this study.

Three patients were found to have a CXCR4 mutation, which involved the C-terminus that contains serine phosphorylation sites that regulate CXCR4 signaling by stromal derived factor-1 $\alpha$  (14). The clinical characteristics and biochemical investigations are summarized in Table 1.

### **Comparison of $^{68}\text{Ga}$ -Pentixafor and $^{18}\text{F}$ -FDG PET/CT**

With the formerly described visual assessment criteria,  $^{68}\text{Ga}$ -Pentixafor PET/CT was visually positive in 17/17 (100%) patients, while  $^{18}\text{F}$ -FDG PET/CT was positive in 10/17 (58.8%) patients. The diagnostic performance of  $^{68}\text{Ga}$ -Pentixafor PET/CT and  $^{18}\text{F}$ -FDG PET/CT in WM/LPL is shown in Table 2.

*Bone Marrow Involvement.* The bone marrow is the predominant site of involvement in WM/LPL, which was confirmed by bone marrow aspiration and biopsy in all recruited patients. According to  $^{68}\text{Ga}$ -Pentixafor and  $^{18}\text{F}$ -FDG PET/CT, bone marrow in the spine, pelvis and appendicular skeleton was affected in all patients; rib involvement

was found in 14 patients; 10 patients had involvement in the skull. In  $^{68}\text{Ga}$ -Pentixafor PET/CT, 10 patients had intense radioactivity in the bone marrow with an SUVmax of  $10.7 \pm 4.1$  (range 6.0-21.3); 6 patients showed moderate uptake in the bone marrow (SUVmax  $4.9 \pm 0.8$ , range 3.7-5.6). Only one patient had mild uptake in the bone marrow (SUVmax 3.9) that was classified as negative according to the visual assessment criteria in this study and showed mildly elevated  $^{68}\text{Ga}$ -Pentixafor uptake in the skull, spine, pelvis, and both the proximal and distal appendicular skeletons, including the carpals and metacarpals. In  $^{18}\text{F}$ -FDG PET/CT, 10 patients had bone marrow uptake with a score of 4, which was classified as positive; the remaining 7 patients had bone marrow intensity with a score of 3 (in 6 patients) and a score of 2 (in 1 patient). The individual SUVmax of bone marrow in both  $^{68}\text{Ga}$ -Pentixafor and  $^{18}\text{F}$ -FDG PET/CT were listed in supplement table 1.

When comparing  $^{68}\text{Ga}$ -Pentixafor with  $^{18}\text{F}$ -FDG, 10 patients had visually higher uptake in the bone marrow with  $^{68}\text{Ga}$ -Pentixafor than with  $^{18}\text{F}$ -FDG PET (example in Fig. 1A); in 6 patients, the intensity of the bone marrow uptake with  $^{68}\text{Ga}$ -Pentixafor and

$^{18}\text{F}$ -FDG PET was comparable, and only 1 patient had higher  $^{18}\text{F}$ -FDG uptake in the bone marrow than  $^{68}\text{Ga}$ -Pentixafor uptake. Regarding the extent of bone marrow involvement,  $^{68}\text{Ga}$ -Pentixafor PET demonstrated more extensive bone marrow disease in 8 patients than  $^{18}\text{F}$ -FDG PET in these individuals (example in Fig. 1B), specifically when visualizing the involvement of the craniofacial bones (in 7 patients) and distal upper extremity bones (in 2 patients). The bone marrow involvement mainly appeared as diffuse bone marrow patterns with homogeneous radioactivity throughout the axial and appendicular skeleton; moreover, additional focal bone marrow lesions were detected by  $^{68}\text{Ga}$ -Pentixafor PET in 3 patients (example in Fig. 2A). Among these 3 patients, only one patient was detected to have focal lesions by  $^{18}\text{F}$ -FDG PET. No bone destruction was found in the coregistered CT. Given the superiority of  $^{68}\text{Ga}$ -Pentixafor to  $^{18}\text{F}$ -FDG in detecting bone marrow involvement, yet we did not find significant correlations between SUVs of bone marrow in baseline  $^{68}\text{Ga}$ -Pentixafor PET and the laboratory results including hemoglobin, serum IgM, M-protein,  $\beta$ 2-microglobulin, serum free light chain, and proportion of lymphoplasmacytic cells in bone marrow biopsy.

*Lymph Node Involvement.* With  $^{68}\text{Ga}$ -Pentixafor PET/CT, 13/17 (76.5%) patients had positive lymph nodes (example in Fig. 2) that involved the neck (9 patients), axilla (7 patients), mediastinum (3 patients), internal mammary (1 patient), hepatoduodenal (11 patients), paraaortic (11 patients), iliac (7 patients), inguinal (7 patients), and epitrochlear (1 patient) nodes. Eight patients had involvement in more than 5 lymph node regions. The maximum size of the positive node in each patient was  $16.5 \pm 7.1$  mm (range 5-26 mm), with a SUVmax of  $8.3 \pm 3.9$  (range 4.0-18.8, supplement table 1). However, with  $^{18}\text{F}$ -FDG PET/CT, only 2 patients were found to have mildly FDG-avid lymph nodes (score 3-4, SUVmax 2.9); moreover,  $^{68}\text{Ga}$ -Pentixafor PET/CT in these 2 patients detected more positive lymph nodes with higher radioactivity than  $^{18}\text{F}$ -FDG PET/CT. No lymph node involvement was detected in 4 patients with either  $^{68}\text{Ga}$ -Pentixafor PET/CT or  $^{18}\text{F}$ -FDG PET/CT.

*Paramedullary Involvement and Involvement of Other Organs.* There was paramedullary disease in 3/17 (17.6%) patients, which affected the soft tissues around the sternum, thoracic vertebrae and presacral space; among these patients, one patient also

had involvement in the thoracic nerve root and sacral nerve root (patient #4, Fig. 2B), which was confirmed by electromyography. The  $^{68}\text{Ga}$ -Pentixafor PET/CT showed intense radioactivity in the paramedullary and nerve root involvement; however, the intensity of FDG uptake was scored as 2-3 in the above lesions, which was much lower than  $^{68}\text{Ga}$ -Pentixafor uptake. The patient with thoracic nerve and sacral nerve root involvement also had central nervous system disease (Bing-Neel syndrome). The  $^{68}\text{Ga}$ -Pentixafor PET/CT in this patient showed markedly increased radioactivity in the bilateral choroid plexus that was not FDG-avid, and the abnormal  $^{68}\text{Ga}$ -Pentixafor uptake in the choroid plexus returned to normal after 6 cycles of chemotherapy. Another 3 patients were found to have splenomegaly with FDG uptake that was scored as 3-4.

### **Follow-up PET/CT after Chemotherapy**

Four patients underwent follow-up  $^{68}\text{Ga}$ -Pentixafor and  $^{18}\text{F}$ -FDG PET/CT after 6-7 cycles of chemotherapy. The intervals between the last cycle of chemotherapy and the PET/CT study were 2 weeks to 3 months. According to the consensus response criteria adopted at the Sixth International Workshop on WM (15), 2 patients with complete



response or very good partial response showed complete remission of the bone marrow and extramedullary involvement on both  $^{68}\text{Ga}$ -Pentixafor and  $^{18}\text{F}$ -FDG PET/CT (example in Fig. 3); another patient with very good partial response only had several remnant CXCR4-positive axillary lymph nodes. The remaining patient who had a partial serological response showed a marked reduction of bone marrow uptake with  $^{68}\text{Ga}$ -Pentixafor and  $^{18}\text{F}$ -FDG (FDG: score 2;  $^{68}\text{Ga}$ -Pentixafor: mild uptake) with complete resolution of the involved lymph nodes.

## DISCUSSION

The diagnosis of diffuse bone marrow involvement of lymphoma with  $^{18}\text{F}$ -FDG PET/CT has always been a clinical dilemma to nuclear medicine physicians. Diffusely increased bone marrow  $^{18}\text{F}$ -FDG uptake is commonly observed in patients with anemia or reactive hyperplasia or those treated with growth factors rather than patients with lymphomatous bone marrow involvement (16,17). Meanwhile,  $^{18}\text{F}$ -FDG PET/CT can miss low-volume involvement (typically < 20% of the marrow) and low-grade lymphoma in bone marrow (16). WM/LPL is an indolent lymphoma that primarily involves the bone

marrow, and anemia is observed in more than 1/3 of WM/LPL patients, which is in part related to B cell infiltration in the bone marrow, blood loss, IgM-associated hemolysis, low erythropoietin levels, or concomitant iron deficiency (18,19). Therefore, bone marrow  $^{18}\text{F}$ -FDG uptake in WM/LPL patients is complicated. In our study, 14/17 (82.4%) patients had anemia (median hemoglobin level 89.5 g/L), which might contribute to the bone marrow activity; in contrast, the percentage of lymphoplasmacytic cells that infiltrated the bone marrow was relatively low – more than 80% of the patients had < 20% marrow infiltration. These factors, and the indolent nature, of course, explained the low sensitivity in detecting bone marrow involvement with  $^{18}\text{F}$ -FDG in WM/LPL patients. In our study, we explored whether  $^{68}\text{Ga}$ -Pentixafor, a PET agent for the in vivo mapping of CXCR4 expression, is superior to  $^{18}\text{F}$ -FDG in diagnosing WM/LPL since there is a high level of CXCR4 expression in the B cells of WM/LPL patients (8,9). We found that  $^{68}\text{Ga}$ -Pentixafor had a higher sensitivity in detecting bone marrow involvement than  $^{18}\text{F}$ -FDG (94.1% vs. 58.8%,  $p = 0.077$ ), although the difference was not significant, which is probably due to the small sample size. The intensity of radioactivity and the

extent of bone marrow involvement shown on PET/CT as well as the ability to detect focal bone marrow lesions with  $^{68}\text{Ga}$ -Pentixafor were also preferable to those with  $^{18}\text{F}$ -FDG.

Lymphadenopathy is reported to occur in approximately 20%-25% of patients with WM/LPL (18,20). With the use of  $^{18}\text{F}$ -FDG PET/CT in our study, the rate of lymph node involvement was consistent with that reported in the literature (positive rate 11.8%, SUVmax 2.9). Surprisingly, with the use of  $^{68}\text{Ga}$ -Pentixafor PET, we noted that most of the lymph node involvement was missed by  $^{18}\text{F}$ -FDG PET. The positive rate of lymph node involvement was significantly higher with  $^{68}\text{Ga}$ -Pentixafor than with  $^{18}\text{F}$ -FDG (76.5% vs. 11.8%,  $p = 0.003$ ) in the recruited WM/LPL patients. Most of the involved lymph nodes showed intense uptake of  $^{68}\text{Ga}$ -Pentixafor (mean SUVmax 8.3, range 4.0-18.8). The most commonly involved lymph nodes were the hepatoduodenal (19%), paraaortic (19%), cervical (16%), axillary (12%), iliac (12%) and inguinal (12%) nodes. Since previous data on lymphadenopathy in WM/LPL were usually based on CT criteria, we believe that the true percentage of lymph node involvement in WM/LPL might be much

higher than the current data suggests, based on the findings of  $^{68}\text{Ga}$ -Pentixafor PET/CT.

Similarly, paramedullary involvement and central nervous system disease showed intense radioactivity with  $^{68}\text{Ga}$ -Pentixafor PET but were negative with  $^{18}\text{F}$ -FDG PET. These results imply that  $^{68}\text{Ga}$ -Pentixafor might be a very promising imaging agent in the diagnosis and staging of WM/LPL.

There might be some limitations of  $^{68}\text{Ga}$ -Pentixafor. First, apart from CXCR4-positive tumor cell infiltration, other activated inflammatory cells in the bone marrow with upregulated CXCR4 expression may also cause increased bone marrow uptake (21-23).

Therefore, the specificity of diagnosing diffuse bone marrow involvement might be hampered when differentiating between different diseases in future studies. Second, due to the lack of histologic verification of lymph node involvement in our study, there might be false positive lymph nodes caused by inflammation, especially the nodes with moderate  $^{68}\text{Ga}$ -Pentixafor uptake and in patients with a limited number of positive nodes.

Third, the incidence of splenic involvement caused by infiltration of clonal cells was reported to be 20%-25% in WM/LPL (18,20). Consistent with the literature,

splenomegaly with mildly increased FDG uptake (uptake > liver) was noted in 17.6% of patients in our study. However, it might be difficult to establish an interpretation criterion to define the high spleen uptake of  $^{68}\text{Ga}$ -Pentixafor as there is considerable physiological uptake in the normal spleen. Finally, in the 4 patients who underwent follow-up PET/CT after chemotherapy, we found an almost complete response with both  $^{68}\text{Ga}$ -Pentixafor and  $^{18}\text{F}$ -FDG PET/CT. However, the surface expression of CXCR4 in tumor cells is a dynamic process that is influenced by therapeutic interventions. Chemotherapy may induce CXCR4 downregulation in multiple myeloma, diffuse large B-cell lymphoma, and acute lymphoblastic leukemia (24,25). If this is also the case in WM/LPL, we must read the images with caution to avoid misinterpreting the tumor response. Moreover, it is important to further investigate the time- and dose-dependent influence of each chemotherapeutic drug on CXCR4 expression in different tumors.

In this study, we found that  $^{68}\text{Ga}$ -Pentixafor PET/CT showed a higher positive rate than  $^{18}\text{F}$ -FDG PET/CT in detecting tumor involvement of the bone marrow, lymph nodes and other extramedullary organs in WM/LPL patients. Further studies are warranted to

clarify the role of  $^{68}\text{Ga}$ -Pentixafor in staging, assessing the response to therapy, and predicting the prognosis of WM/LPL patients.

#### **DISCLOSURE:**

This work was supported by the National Natural Science Foundation of China (81701741), the CAMS Initiative for Innovative Medicine (CAMS-I2M, 2017-I2M-3-001), and the Fundamental Research Funds for the Central Universities, the Young Scientific Research Fund of PUMC (2017320004). No other potential conflicts of interest that are relevant to this article exist.

## **KEY POINTS:**

**QUESTION:** Is  $^{68}\text{Ga}$ -Pentixafor PET/CT superior to  $^{18}\text{F}$ -FDG PET/CT in detecting tumor involvement in WM/LPL?

**PERTINENT FINDINGS:** In our prospective cohort study of 17 patients with WM/LPL,  $^{68}\text{Ga}$ -Pentixafor PET/CT showed a higher positive rate than  $^{18}\text{F}$ -FDG PET/CT in detecting bone marrow involvement, lymph node involvement and other extramedullary involvement.

**IMPLICATIONS FOR PATIENT CARE:**  $^{68}\text{Ga}$ -Pentixafor PET/CT might be a promising tool in the assessment of WM/LPL.

## REFERENCES:

1. Cheson BD, Fisher RI, Barrington SF, Cavalli F, Schwartz LH, Lister TA.

Recommendations for initial evaluation, staging, and response assessment of Hodgkin

and non-Hodgkin lymphoma: the Lugano classification. *J Clin Oncol.*

2014;32:3059-3068.

2. Banwait R, O'Regan K, Campigotto F, et al. The role of 18F-FDG PET/CT imaging

in Waldenstrom macroglobulinemia. *Am J Hematol.* 2011;86:567-572.

3. Teicher BA, Fricker SP. CXCL12 (SDF-1)/CXCR4 pathway in cancer. *Clin Cancer*

*Res.* 2010;16:2927-2931.

4. Philipp-Abbrederis K, Herrmann K, Knop S, et al. In vivo molecular imaging of

chemokine receptor CXCR4 expression in patients with advanced multiple myeloma.

*EMBO Mol Med.* 2015;7:477-487.

5. Wester HJ, Keller U, Schottelius M, et al. Disclosing the CXCR4 expression in

lymphoproliferative diseases by targeted molecular imaging. *Theranostics.*

2015;5:618-630.



6. Herhaus P, Habringer S, Philipp-Abbrederis K, et al. Targeted positron emission tomography imaging of CXCR4 expression in patients with acute myeloid leukemia. *Haematologica*. 2016;101:932-940.
  
7. Lapa C, Schreder M, Schirbel A, et al. [(68)Ga]Pentixafor-PET/CT for imaging of chemokine receptor CXCR4 expression in multiple myeloma - comparison to [(18)F]FDG and laboratory values. *Theranostics*. 2017;7:205-212.
  
8. Ngo HT, Leleu X, Lee J, et al. SDF-1/CXCR4 and VLA-4 interaction regulates homing in Waldenstrom macroglobulinemia. *Blood*. 2008;112:150-158.
  
9. Hunter ZR, Yang G, Xu L, Liu X, Castillo JJ, Treon SP. Genomics, signaling, and treatment of Waldenstrom macroglobulinemia. *J Clin Oncol*. 2017;35:994-1001.
  
10. Luo Y, Pan Q, Feng J, Cao X, Li F. Chemokine receptor CXCR4-targeted PET/CT with <sup>68</sup>Ga-Pentixafor shows superiority to <sup>18</sup>F-FDG in a patient with Waldenstrom macroglobulinemia. *Clin Nucl Med*. 2018;43:548-550.
  
11. Nanni C, Versari A, Chauvie S, et al. Interpretation criteria for FDG PET/CT in multiple myeloma (IMPeTUs): final results. IMPeTUs (Italian myeloma criteria for PET

USE). *Eur J Nucl Med Mol Imaging*. 2018;45:712-719.

12. Morel P, Duhamel A, Gobbi P, et al. International prognostic scoring system for

Waldenstrom macroglobulinemia. *Blood*. 2009;113:4163-4170.

13. Treon SP, Xu L, Yang G, et al. MYD88 L265P somatic mutation in Waldenstrom's

macroglobulinemia. *N Engl J Med*. 2012;367:826-833.

14. Hunter ZR, Xu L, Yang G, et al. The genomic landscape of Waldenstrom

macroglobulinemia is characterized by highly recurring MYD88 and WHIM-like CXCR4

mutations, and small somatic deletions associated with B-cell lymphomagenesis. *Blood*.

2014;123:1637-1646.

15. Treon SP. How I treat Waldenstrom macroglobulinemia. *Blood*. 2015;126:721-732.

16. Barrington SF, Mikhaeel NG, Kostakoglu L, et al. Role of imaging in the staging and

response assessment of lymphoma: consensus of the International Conference on

Malignant Lymphomas Imaging Working Group. *J Clin Oncol*. 2014;32:3048-3058.

17. Adams HJ, Nievelstein RA, Kwee TC. Opportunities and limitations of bone marrow

biopsy and bone marrow FDG-PET in lymphoma. *Blood Rev*. 2015;29:417-425.

18. Kapoor P, Paludo J, Vallumsetla N, Greipp PR. Waldenstrom macroglobulinemia: What a hematologist needs to know. *Blood Rev.* 2015;29:301-319.
19. Mazzucchelli M, Frustaci AM, Deodato M, Cairoli R, Tedeschi A. Waldenstrom's macroglobulinemia: an update. *Mediterr J Hematol Infect Dis.* 2018;10:e2018004.
20. Ghobrial IM, Gertz MA, Fonseca R. Waldenstrom macroglobulinaemia. *Lancet Oncol.* 2003;4:679-685.
21. Cytawa W, Kircher S, Schirbel A, et al. Chemokine receptor 4 expression in primary Sjogren's syndrome. *Clin Nucl Med.* 2018;43:835-836.
22. Derlin T, Gueler F, Brasen JH, et al. Integrating MRI and chemokine receptor CXCR4-targeted PET for detection of leukocyte infiltration in complicated urinary tract infections after kidney transplantation. *J Nucl Med.* 2017;58:1831-1837.
23. Margaritopoulos GA, Antoniou KM, Lasithiotaki I, Proklou A, Soufla G, Siafakas NM. Expression of SDF-1/CXCR4 axis in bone marrow mesenchymal stem cells derived from rheumatoid arthritis-usual interstitial pneumonia. *Clin Exp Rheumatol.* 2013;31:610-611.

24. Lapa C, Herrmann K, Schirbel A, et al. CXCR4-directed endoradiotherapy induces high response rates in extramedullary relapsed multiple myeloma. *Theranostics*. 2017;7:1589-1597.
25. Lapa C, Luckerath K, Kircher S, et al. Potential influence of concomitant chemotherapy on CXCR4 expression in receptor directed endoradiotherapy. *Br J Haematol*. 2019;184:440-443.

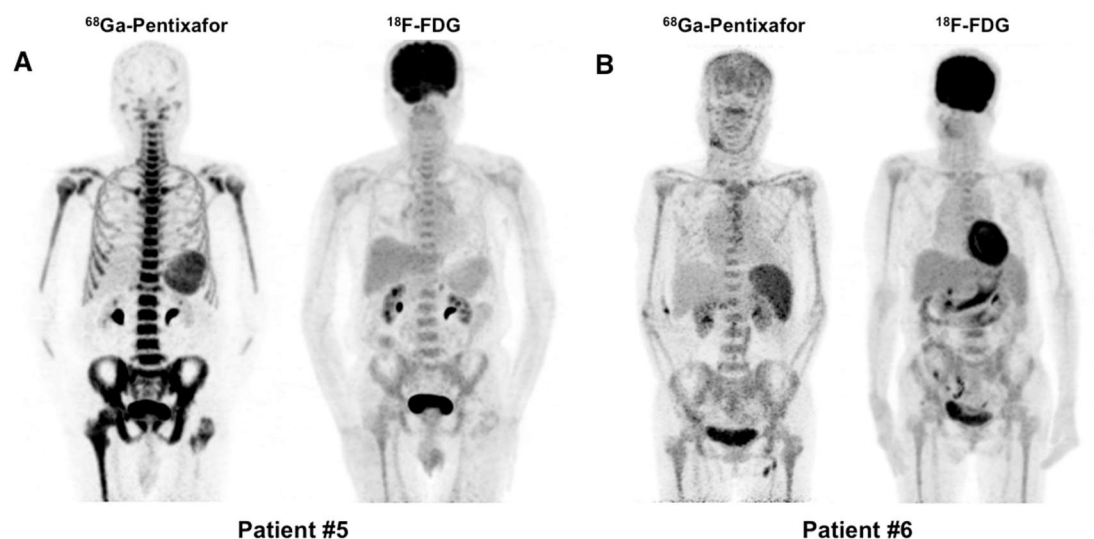


FIGURE 1. Examples of <sup>68</sup>Ga-Pentixafor and <sup>18</sup>F-FDG PET in patients with WM/LPL. (A) Patient #5 had relapsed WM (IgM  $\kappa$ ), had an ISS-WM score of 4, and was classified as high risk. The <sup>68</sup>Ga-Pentixafor showed intense radioactivity in the bone marrow that was much higher than <sup>18</sup>F-FDG (score 3). (B) Patient #6 had WM (IgM  $\kappa$ ) and secondary amyloidosis in the myocardium, had an ISS-WM score of 3, and was classified as high risk. The intensity of <sup>68</sup>Ga-Pentixafor and <sup>18</sup>F-FDG uptake in bone marrow was comparable, but the bone marrow involvement was more extensive with <sup>68</sup>Ga-Pentixafor than with <sup>18</sup>F-FDG. Additional bone marrow disease was detected in the craniofacial bones, ulna, radius, carpals and metacarpals with <sup>68</sup>Ga-Pentixafor. Note that the submandibular, retroperitoneal and inguinal lymph nodes were positive on <sup>68</sup>Ga-Pentixafor PET, but these lymph nodes were not FDG-avid.

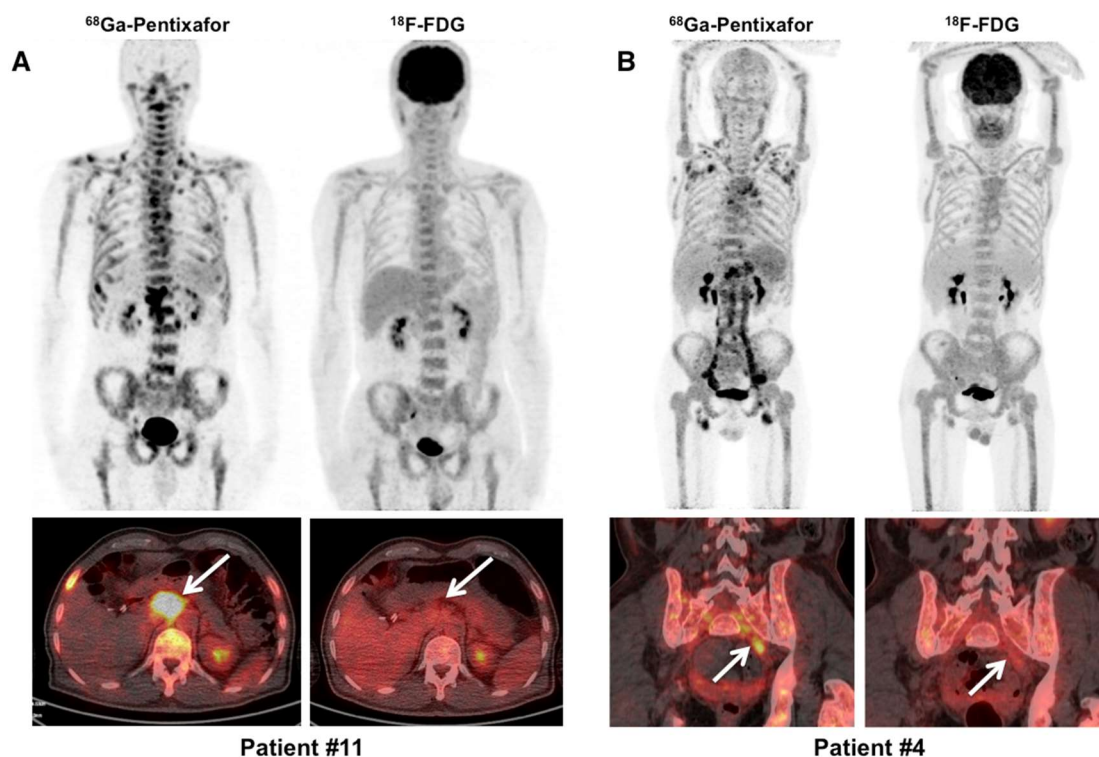


FIGURE 2. (A) Patient #11 had WM (IgM  $\lambda$ ), had an ISS-WM score of 2, and was classified as indeterminate risk. The  $^{68}\text{Ga}$ -Pentixafor showed intense radioactivity in the bone marrow with multiple focal lesions and CXCR4-positive lymph nodes (arrow). The FDG activity (score 4) was homogeneously distributed in the bone marrow, and the lymph nodes were not FDG-avid (arrow). (B) Patient #4 had WM (IgM  $\kappa$ ) and Bing-Neel syndrome, had an ISS-WM score of 2, and was classified as indeterminate risk. Multiple CXCR4-positive lymph nodes were detected in the neck, axilla, hepatoduodenal, retroperitoneal, iliac, and inguinal regions, and most of these lymph nodes were missed with  $^{18}\text{F}$ -FDG PET. The involved left iliac nerve root (arrow) was CXCR4-positive but not FDG-avid.

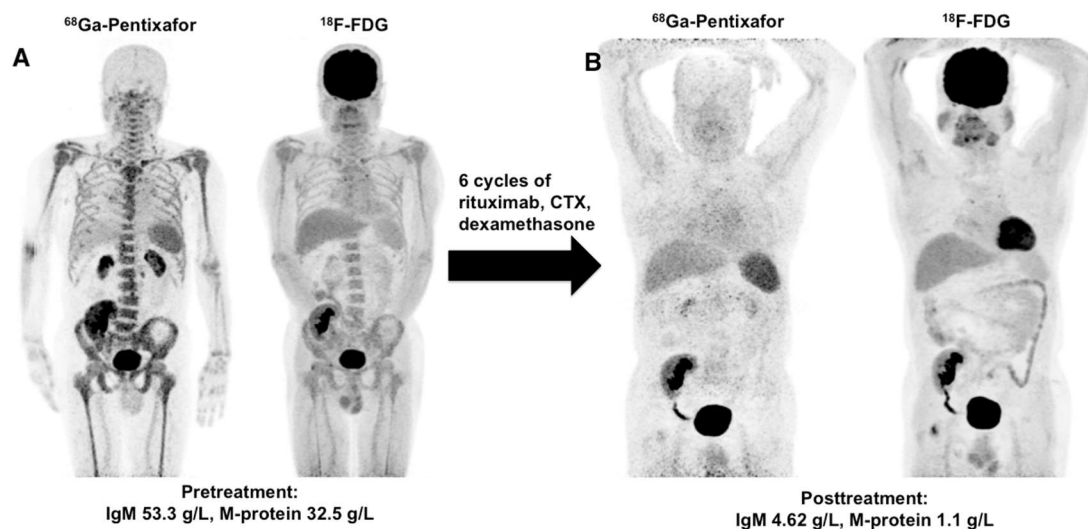


FIGURE 3. Patient #12 had WM (IgM  $\kappa$ ), had an ISS-WM score of 2, and was classified as indeterminate risk. (A) Pretreatment <sup>68</sup>Ga-Pentixafor and <sup>18</sup>F-FDG PET/CT showed diffuse involvement in the bone marrow. There was also lymph node involvement in the neck, mediastinum, hepatoduodenal, retroperitoneal, and inguinal regions, as depicted on <sup>68</sup>Ga-Pentixafor PET/CT. (B) Posttreatment <sup>68</sup>Ga-Pentixafor and <sup>18</sup>F-FDG PET/CT performed 2 weeks after the completion of 6 cycles of chemotherapy showed complete remission of the bone marrow and lymph node diseases on both the <sup>68</sup>Ga-Pentixafor and <sup>18</sup>F-FDG PET/CT. The serum IgM and M-protein levels were markedly decreased compared with those at baseline.

TABLE 1. The patients' clinical characteristics and biochemical investigation results

No.	Age /sex	ISS-WM*	Cytogenetics†	M-pro type	IgM (g/L)	M-pro (g/L)	β2MG (mg/L)	sFLC (mg/L)
1	69/M	high	MYD88 <sup>L265P</sup>	IgM λ	66.99	47.7	9.54	n/a
2	69/F	high	MYD88 <sup>L265P</sup>	IgM κ	28.93	17.5	4.85	64.7(κ)
3	56/M	high	MYD88 <sup>L265P</sup>	IgM κ	25.32	13.1	9.28	33.8(κ)
4	61/M	IND	MYD88 <sup>L265P</sup>	IgM κ	30.49	18.5	6.13	637.5(κ)
5	87/M	high	MYD88 <sup>L265P</sup>	IgM κ	4.19	1.1	3.68	16.2(κ)
6	78/F	high	MYD88 <sup>L265P</sup>	IgM κ	18.81	10.8	12.8	365.0(κ)
7	72/M	high	MYD88 <sup>L265P</sup>	IgM κ	5.78	2.1	8.93	1629.1(κ)
8	56/F	IND	MYD88 <sup>L265P</sup>	IgM λ	62.43	34.3	3.06	n/a
9	72/M	IND	MYD88 <sup>L265P</sup>	IgM λ	15.2	10.5	3.27	27.2(λ)
10	60/M	low	MYD88 <sup>L265P</sup> CXCR4 <sup>s338x</sup>	IgM λ	42.91	25.3	2.34	172.5(λ)
11	64/M	IND	MYD88 <sup>L265P</sup>	IgM λ	23.69	10.6	5.71	151.3(λ)
12	64/M	IND	MYD88 <sup>L265P</sup>	IgM κ	53.3	32.5	5.27	159.0(κ)
13	48/F	n/a ‡	MYD88 <sup>L265P</sup> CXCR4 <sup>s338x</sup>	IgD κ	6.67 (IgD) §	n/a	n/a	527.5(κ)
14	55/F	low	MYD88 <sup>L265P</sup> CXCR4 <sup>s338x</sup>	IgM κ	82.49	35.6	2.93	25.7(κ)
15	52/F	IND	MYD88 <sup>L265P</sup>	IgM κ	38.13	21.6	3.34	99.4(κ)
16	53/M	IND	MYD88 <sup>L265P</sup>	IgM λ	20.13	13.9	3.57	89.2(λ)
17	48/M	high	MYD88 <sup>L265P</sup>	IgM κ	77.67	47.4	6.6	6.5(κ)

\* The ISS-WM prognostic scoring system includes: age > 65 yr, β2MG >3 mg/L, hemoglobin ≤11.5 g/dL, platelet ≤ 100×10<sup>9</sup>/L, and IgM >7 g/dL. Low risk: ≤ 1 adverse characteristic and age ≤ 65 yr; high risk: ≥3 adverse characteristics; indeterminate risk: 2 adverse characteristics or age > 65 yr.

†MYD88 and CXCR4 warts, hypogammaglobulinemia, infections, myelokathexis syndrome-like somatic mutations were tested.

‡The ISS-WM scoring system was not applicable in IgD-type WM/LPL.

§Serum IgD level was measured as IgD type M-protein level.



ISS-WM = international staging system for WM; M-pro = M protein;  $\beta$ 2MG =  $\beta$ 2-microglobulin; sFLC = serum free light chain; n/a = not applicable; IND=indeterminate.

TABLE 2. Diagnostic performance of  $^{68}\text{Ga}$ -Pentixafor and  $^{18}\text{F}$ -FDG PET/CT

	$^{68}\text{Ga}$ -Pentixafor	$^{18}\text{F}$ -FDG	<i>P</i> value
PET-positive patients	17/17 (100%)	10/17 (58.8%)	0.023*
Bone marrow involvement	16/17 (94.1%)	10/17 (58.8%)	0.077
Lymph node involvement	13/17 (76.5%)	2/17 (11.8%)	0.003*
Paramedullary involvement	3/17 (17.6%)	0/17 (0%)	0.248
CNS involvement	1/17 (5.9%)	0/17 (0%)	1.0

$^{68}\text{Ga}$ -Pentixafor: positive is defined by uptake > liver;  $^{18}\text{F}$ -FDG: positive is defined by uptake  $\geq$  score 4 (5-point scale).

\* The difference in the positive rate between  $^{68}\text{Ga}$ -Pentixafor and  $^{18}\text{F}$ -FDG is significant.

Supplement Table 1. SUVmax of bone marrow and lymph nodes in PET/CT

No.	Bone marrow SUVmax		Lymph node SUVmax	
	<sup>68</sup> Ga-Pentixafor	<sup>18</sup> F-FDG	<sup>68</sup> Ga-Pentixafor	<sup>18</sup> F-FDG
1	3.8	2.0	NA	NA
2	21.3	5.6	9.1	2.0
3	3.9	3.4	7.7	not seen
4	6.7	2.8	12.5	2.9
5	13.2	2.2	NA	NA
6	5.6	3.4	6.4	not seen
7	5.4	3.2	6.1	not seen
8	3.7	2.6	4.5	not seen
9	5.6	2.1	NA	NA
10	11.1	2.0	4.2	not seen
11	11.0	3.5	18.8	not seen
12	8.6	3.1	7.3	not seen
13	6.0	4.1	4.0	not seen
14	8.1	4.2	6.7	not seen
15	5.1	2.1	NA	NA
16	11.7	2.8	9.9	not seen
17	9.5	3.9	10.9	not seen

NA = not applicable



The Journal of  
NUCLEAR MEDICINE

## **$^{68}\text{Ga}$ -pentixafor PET/CT for imaging of chemokine receptor-4 expression in Waldenström macroglobulinemia/lymphoplasmacytic lymphoma: comparison to $^{18}\text{F}$ -FDG PET/CT**

Yaping Luo, Xinxin Cao, Qingqing Pan, Jian Li, Jun Feng and Fang Li

*J Nucl Med.*

Published online: May 17, 2019.

Doi: 10.2967/jnumed.119.226134

---

This article and updated information are available at:

<http://jnm.snmjournals.org/content/early/2019/05/17/jnumed.119.226134>

---

Information about reproducing figures, tables, or other portions of this article can be found online at:

<http://jnm.snmjournals.org/site/misc/permission.xhtml>

Information about subscriptions to JNM can be found at:

<http://jnm.snmjournals.org/site/subscriptions/online.xhtml>

---

*JNM* ahead of print articles have been peer reviewed and accepted for publication in *JNM*. They have not been copyedited, nor have they appeared in a print or online issue of the journal. Once the accepted manuscripts appear in the *JNM* ahead of print area, they will be prepared for print and online publication, which includes copyediting, typesetting, proofreading, and author review. This process may lead to differences between the accepted version of the manuscript and the final, published version.

---

*The Journal of Nuclear Medicine* is published monthly.  
SNMMI | Society of Nuclear Medicine and Molecular Imaging  
1850 Samuel Morse Drive, Reston, VA 20190.  
(Print ISSN: 0161-5505, Online ISSN: 2159-662X)

© Copyright 2019 SNMMI; all rights reserved.

The logo for the Society of Nuclear Medicine and Molecular Imaging (SNMMI) consists of the letters 'S', 'N', 'M', and 'I' arranged in a 2x2 grid, each within its own red square. To the right of this graphic, the full name of the society is written in a sans-serif font.  
SOCIETY OF  
NUCLEAR MEDICINE  
AND MOLECULAR IMAGING